Big Time-Series Data Analytics in Structural Health Monitoring at the Acropolis of Athens Utilising Optical Fibre Sensors

E. Kapogianni[1], G. Sakellariou[2], and M. Sakellariou[3]

[1]*Dr, National Technical University of Athens, Greece, email: elkapogianni@mail.ntua.gr*

[2]*Dr, Independent Researcher, email: georgios.sakellariou@gmail.com*

[3]*Professor Emeritus, National Technical University of Athens, Greece, email: mgsakel@mail.ntua.gr*

ABSTRACT

The Acropolis of Athens is one of the most iconic ancient Greek monumental complexes still preserved today. Among its monuments, such as the *Parthenon*, the *Erechtheion*, the *Propylaia*, and the *Arrephorion*, the ancient *Circuit Wall* stands out as a key geotechnical element. This masonry retaining structure, composed of mixed marble and stone, surrounds and supports the Acropolis Hill plateau, functioning as a gravity wall that ensures overall stability. Due to the site's prolonged environmental exposure and seismic vulnerability, the Wall has experienced various loading conditions over time, resulting in notable structural degradation. To assess and monitor its condition, an advanced structural health monitoring system employing Fiber Bragg Grating sensors was installed. The monitoring system comprised eight optical fibre strain sensors mounted on four smart rods (with inner and outer configurations), two temperature sensors installed on a separate rod for thermal compensation, and one acceleration sensor installed on the Wall. The sensors were connected in series and parallel configurations to optimise signal integrity and data transmission efficiency. Measurements were continuously recorded over several months, producing very large datasets that demanded specialised processing and analysis methods. Raw sensor data were systematically ingested using custom data pipelines implemented in R, a programming language and environment for statistical computing, data analysis and visualisation, organised into conformed and unified datasets, and cleaned to ensure quality and consistency. The resulting time series were transformed to enable visualisation and efficiently stored to support further analysis and long-term insight extraction. Overall, the study demonstrates the effectiveness of optical fibre sensing for heritage preservation, providing reliable, trend analysis insights into structural behaviour, and establishing a scalable framework for monitoring other culturally significant monuments exposed to similar stress patterns.

Keywords: Cultural Heritage Preservation; Acropolis of Athens; Masonry Retaining Wall; Structural Health Monitoring; Optical Fibre Sensors; Big Data Analysis; Data Modelling, Descriptive Analytics

INTRODUCTION

The Acropolis Hill rises approximately 150 m above sea level and 70 m above the city of Athens, exhibiting a trapezoidal shape with dimensions of roughly 300 m in length and 150 m in width and is located approximately 2 km southwest of Lycabettus Hill (Higgins & Higgins, 1996). Geologically, the Hill is primarily composed of limestone overlying the Athenian Schist (Koukis et al., 2015; Trikkalinos, 1977). The limestone is largely visible where artificial embankments have not been constructed, particularly on the south side, where embankments were added to create a levelled surface (Figure 1). The Athenian Schist is exposed at the main archaeological entrance and less frequently elsewhere. Karstification within the limestone has led to the formation of cavities that facilitate water flow, promoting erosion and localized rockfall phenomena. Furthermore, the Acropolis Hill has been affected by several regional earthquakes over the centuries (Ambraseys, 2010; Zambas et al., 2011). In general, the seismic response of the monuments has been relatively moderate, with structural damages mostly resulting from human interventions, environmental pollution, and inefficient past rehabilitation rather than direct earthquake impacts.

The Acropolis Circuit Wall is an irregular masonry retaining wall, approximately 800 m in length and varying in height between 5 and 18 m. It is mainly composed of marble and small stones, with later repairs introducing mixed courses. Over centuries, the Wall has been subjected to extreme weather, variable loads, human interventions, and seismic activity, resulting in cracks, block falls, and displacements. The south part of the Wall, reaching its greatest height (~18 m), retains relatively poorly compacted backfill and exhibits visible cracks, particularly at the south-east corner, which is frequently used for transporting heavy restoration materials, increasing its vulnerability.

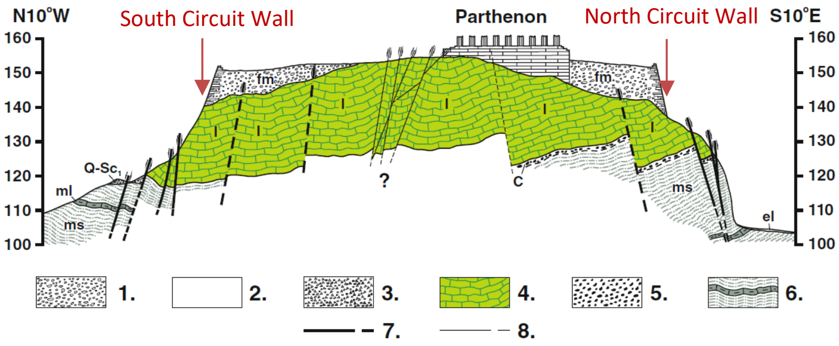

Figure 1. *Geological section of the Acropolis Hill. 1: artificial earthfill (fm), 2: eluvial mantle (el), 3: talus (Q-Sc), 4: limestone (l), 5: conglomerates (C), 6: schist-sandstones-marl series (ms-ml), 7: fault, 8: main fractures on the Acropolis plateau (after Koukis et al., 2015).*

Given the combination of structural complexities, geological conditions, long-term weathering, and human-induced impacts described above, the implementation of instrumented structural monitoring systems has emerged as a necessary component of structural evaluation. Such systems now represent a key scientific approach for assessing the condition and behaviour of critical, historical, and high-risk structures. More specifically, modern monitoring aims to create “intelligent” structures, such as bridges, buildings, and geotechnical constructions, equipped with sensors that provide real-time information at multiple locations, enabling early detection of structural defects. Among the most effective techniques, optical fibre (o.f.) sensors have increasingly replaced conventional instrumentation over the past decade due to their high precision, mechanical robustness, and small size (Bado & Casas, 2021; Soga et al., 2015). The extensive deployment of sensors and the continuous real-time monitoring of structural behaviour often generate a substantial volume of high-resolution data. Effectively managing, processing, and analysing this large dataset is essential to extract meaningful information on structural performance, detect anomalies, and support informed decision-making for preservation and maintenance. This highlights the importance of developing systematic approaches and methodologies capable of handling complex, multi-sensor data streams while ensuring accurate interpretation of the structural response under varying environmental and operational conditions.

1. OPTICAL FIBRE SENSOR DEPLOYMENT

An optical fibre consists of a glass core surrounded by a cladding of differing refractive index and is coated with a protective polymer layer to prevent mechanical damage, moisture-induced weakening, and crack propagation. A Fibre Bragg Grating (FBG) sensor is a specially treated portion of the fibre that reflects a narrow wavelength band of light while transmitting the remainder. The reflected wavelength shifts in response to strain, temperature or acceleration changes. By placing FBG sensors at critical locations within a structure and recording the reflected wavelength with appropriate interrogators, precise measurements of structural deformations can be obtained. Optical fibre sensors combine microstrain-level precision, mechanical robustness, signal multiplexing, and small size, allowing flexible placement on a wide variety of structures (Kapogianni & Sakellariou, 2025).
As mentioned above, a comprehensive optical fibre monitoring system was installed on the southern part of the Acropolis Circuit Wall, to capture strain, temperature, and acceleration variations (Kapogianni et al., 2019; Sakellariou et al., 2016; Kapogianni et al., 2016). The South Wall was selected as the focus for the deployment of the optical fibre array due to its structural importance. This section corresponds to one of the tallest segments of the Circuit Wall (~18 m) and retains a substantial volume of backfill, making it structurally critical. Cracks present in this section indicate localized structural weaknesses that require careful observation. Furthermore, the area is in close proximity to pre-existing accelerographs, which are part of the Acropolis Hill accelerographic network (Kalogeras et al., 2010; Kapogianni et al., 2021). The selection also facilitates future integration of o.f. measurements with accelerographic data, enabling comprehensive multi-sensor monitoring. Figure 2 illustrates the positions of the Sensors on the South Wall, providing a clear overview of the monitoring layout.

Figure 2. *Positions of the sensors installed on the Circuit Wall, illustrating the overall monitoring layout.*

More specifically, the array included four Smart Rods, each equipped with two strain sensors (located at the inner and outer sides of the Rods) to evaluate local and global curvature changes, as well as a separate Rod carrying two temperature sensors for thermal compensation. A single-axis FBG acceleration sensor (Smart Accel - LF) was also included to detect low-frequency vibrations. All sensors were mounted on stainless steel plates without adhesive to allow repositioning if required, and optical signals were transmitted via an Optical Sensing Interrogator. The fibres were connected in series, parallel, or combined configurations, with splicing performed in the field and at the laboratory to ensure robust signal acquisition. In Figure 3, part of the equipment installed on the south Circuit Wall is shown (left), and the system installation location (right). The system provided continuous measurements over a 24-month period, with data from strain and temperature sensors recorded at a frequency of one measurement per second, generating a high-resolution dataset. In total, ten strain and temperature sensors were active, continuously recording the structural response of the Wall under varying environmental conditions and producing a substantial volume of data.

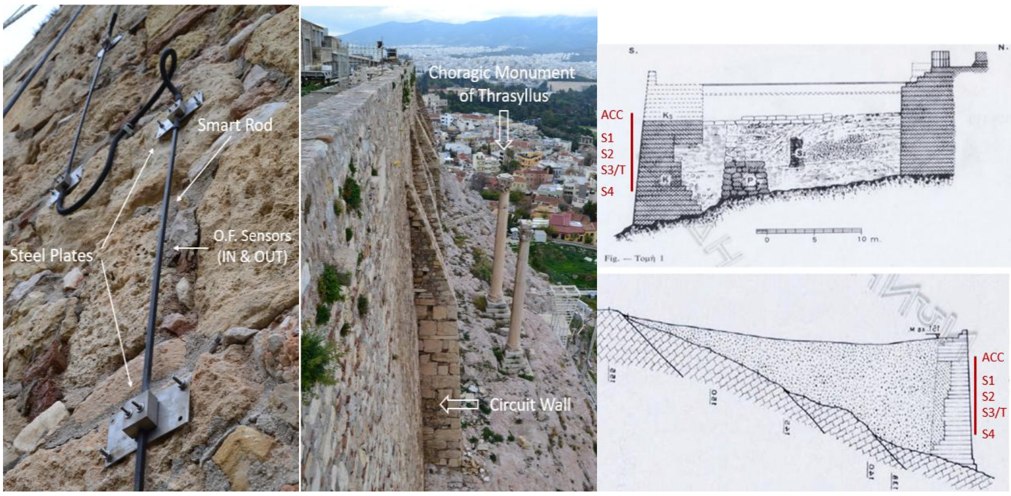

Figure 3. *Part of the equipment installed on the south Circuit Wall (left), location of the system installation (middle), and cross-sections of the southern part of the Circuit Wall (right) after Trikkalinos (1977).*

For each strain sensor, the wavelength variation can be calculated as the difference between the current value and the initial / reference value:

$$\Delta\lambda = \lambda_{current} - \lambda_{reference} \quad (1)$$

For the temperature sensors, the temperature variation is computed using:

$$\Delta T = (1000 \cdot \Delta\lambda) / K_t \quad (2)$$

where K_t = 10.1 pm/°C is the temperature-wavelength coefficient, and the factor 1000 converts nanometres (nm) to picometres (pm). The resulting temperature variations in °C can then be recorded in the dataset.

Strain ($\Delta\varepsilon$) is derived from the wavelength variation with thermal compensation according to:

$$\Delta\varepsilon = (\Delta\lambda - K_t \cdot \Delta T) / K_\varepsilon \quad (3)$$

where K_ε = 1.2 pm/μstrain is the strain-wavelength coefficient for the sensors used in this study. Substituting the coefficient values and expressing $\Delta\lambda$ in nanometres, the equation becomes:

$$\Delta\varepsilon = (1000 \cdot (\Delta\lambda - 10.1 \cdot \Delta T)) / 1.2 \quad (4)$$

This formulation allows accurate conversion of wavelength changes into strain values while accounting for thermal effects.

The equations described above enable the conversion of raw wavelength measurements into temperature-compensated strain values. However, their application to long-term monitoring data raises several issues that require further examination, including the influence of temperature and the effectiveness of the applied thermal correction. The vertical sensor distribution may also highlight locations with more critical structural behaviour. In addition, differences between inner and outer sensors should be assessed, as they may capture local curvature effects. Finally, the large volume of generated data presents a processing and interpretation challenge, requiring robust data management strategies.

2. PROGRAMMATIC BIG DATA ANALYSIS

High-frequency monitoring generates substantial data volumes that demand significant processing power to yield timely insights while avoiding data sprawl. For this study, the dataset analysed contained time-series data exported in raw text format from optical fibre sensors, capturing readings from 10 sensors every second over a period of 2 years. Nearly 63 million rows comprising 630 million data points rendered conventional tools inadequate, necessitating a custom pipeline for long-range trend analysis. To reduce time-to-insight, the authors developed a custom R-based data pipeline tailored for high-frequency analysis (Henderson & Fulcher, 2022). R's interactive console and specialised time-series libraries (Shumway & Stoffer, 2017) facilitated the rapid experimentation and visualisation required for this research. Data ingestion and preparation involved a custom script that parsed exported sensor data text files (2 files per day of readings on average), collated by binding into a single data frame and performed in-memory data cleansing. This process resulted in data frames of approximately 2.6M rows containing 260M meaningful data points in tabular format for each month of uninterrupted measurements. Once ingested, calculations to derive temperature-corrected strain measurements according to formulas presented elsewhere in this paper followed, using vector operations wherever possible. Next, calculated time-series tables were resampled to reduce the number of data points for visualisation. This was achieved by aggregating data over 20-minute windows and computing a moving average within each interval. Lastly, data was serialised into block storage to optimise efficiency and accessibility. This approach reduced storage footprints while increasing ingestion throughput by an order of magnitude; it establishes a robust framework for future research involving larger datasets and more complex analytical modelling.

3. FROM DATA TO INSIGHTS

To explore the behaviour of the eight strain sensors and to evaluate the influence of temperature, sensor position, and long-term effects, a series of visualisations was produced. The first level of analysis focuses on short-term fluctuations, using 24-hour plots that display measurements at 20-minute intervals for all sensors, both with and without thermal compensation. These plots reveal the immediate daily dynamics of the system and clearly show that thermal compensation is essential, as uncorrected values appear artificially increased. Moving to a broader timescale, monthly comparisons were generated for the first month of recordings, distinguishing between the four "in" and four "out" sensors to investigate how the location on the Circuit Wall influences the recorded strain response. The differences between "in" and "out" strain measurements reflect deformation on opposite sides of the smart rod and indicate local bending behaviour, while also suggesting a combined effect associated with pre-existing cracks. In this context, the inner side appears to capture transverse expansion of the structure, including joints and cracks, resulting in higher elongation values. The near-zero nighttime readings further indicate that these strains are reversible, as the wall is unloaded from daytime loads. To capture intermediate and long-term trends, additional plots were produced for multi-month periods, which confirm a gradual increase in strain over time. Finally, interannual comparisons of June 2016 and June 2017 recordings were developed for each sensor, showing slightly higher strain values one year later and providing a direct means of detecting long-term behaviour. These visualisations provide a comprehensive framework for understanding the role of sensor placement, and the significance of thermal effects, while also enabling the evaluation of long-term structural changes. More specifically, Figure 4a and b, shows plots created using four sensors in the IN positions and four sensors in the OUT positions for a 24-hour period, without applying any temperature correction. The results showed that on the external side, Sensor 4 exhibited the highest strain, while Sensor 1 recorded the lowest. On the internal side, which is attached to the wall, Sensor 2 showed the highest strain levels, whereas Sensor 4 recorded the lowest. A noticeable increase in strain was observed during a specific period, from early morning to midday, which is attributed both to the rise in ambient temperature and to increased visitor activity at the Archaeological Site during those hours. Subsequently, the influence of temperature was incorporated, and two additional plots were produced (Figures 5a & b). It became evident that temperature correction is essential, as the uncorrected strain values appear artificially elevated. Therefore, strain-monitoring installations in the field should include temperature sensors so that the thermal component can be removed. After this point, all further analyses and plots were generated with temperature-corrected data.

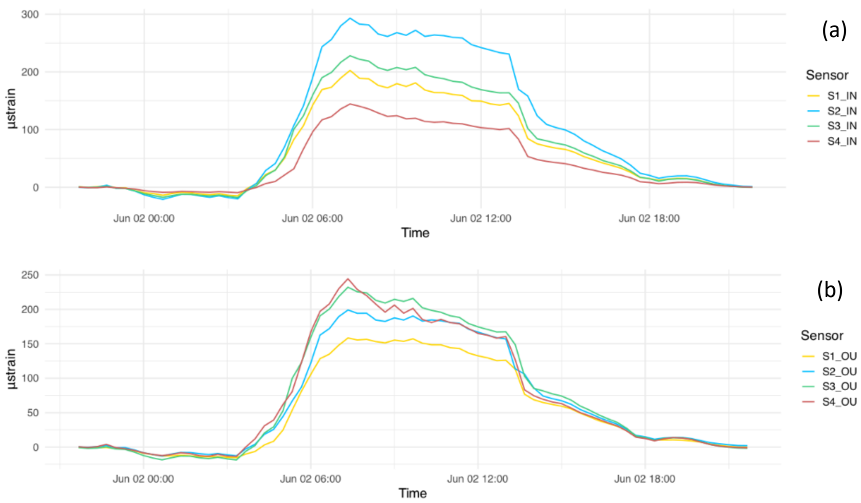

Figure 4. *Sensors on the inner (a) and outer (b) sides of the Smart Rods without thermal compensation.*

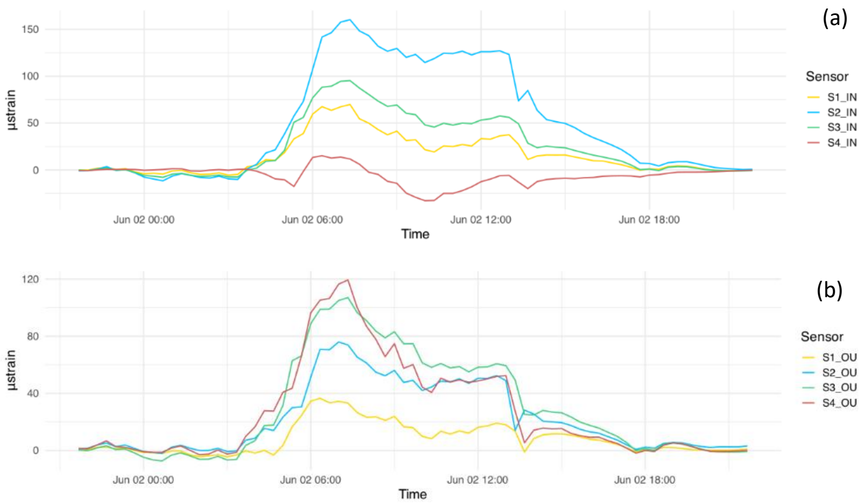

Figure 5. *Sensors on the inner (a) and outer (b) sides of the Smart Rods with thermal compensation.*

A month-long comparison was subsequently carried out using the full dataset from the system's first month of operation, examining IN and OUT positions separately as shown in Figures 6a and b. For the internal sensors, Sensor 2 consistently displayed the highest strain values throughout the entire month. In contrast, the external sensors did not show significant long-term differentiation. Although Sensor 4 initially appeared to experience higher strain, this pattern did not persist throughout the month. This finding highlights that conclusions should not be drawn solely from short time windows-such as a single-day plot-but rather from extended monitoring periods. For example, although the 24-hour plot suggested that external Sensor 4 carries the highest strain, the month-long dataset does not confirm this. Additionally, it is estimated that the sudden increase on the plots for a small period of time, appears only because missing measurements hide the intermediate values that would have shown a gradual rise.

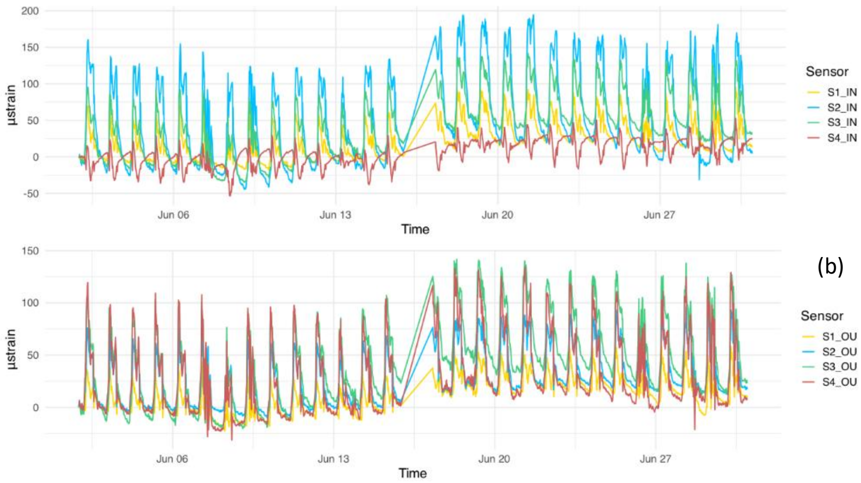

Figure 6. *Month-long strain comparison for the inner (a) and outer (b) sensors.*

Furthermore, a detailed investigation was conducted for each individual sensor in both the internal and external positions over the same monthly period (Figures 7a to 7d). The results show that Sensor 2 (S2) presents the greatest variation on the internal side, consistent with previous observations and Sensor 3 (S3) exhibits the smallest variation. For Sensor 4 (S4), however, the greater fluctuation appears on the external side rather than the internal one, meaning that higher strain levels are observed externally. These distinctions between sensors and positions demonstrate how local structural behaviour can differ substantially within the same monitoring system. The observed variation between the upper and lower sensors reflects a non-uniform deformation profile along the wall height, fully consistent with the static behaviour of the structural element. The structure consists of a retaining wall with buttresses, which extends from position S3 downward, resulting in greater mobility of the upper part of the wall compared to the lower part. This effect is further amplified since it functions as a retaining wall, with the S4 sensors located near the base, which acts as a fixed support.

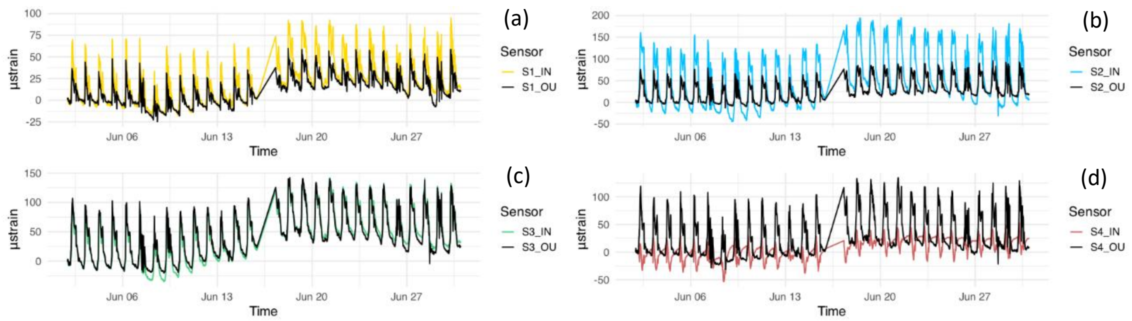

Figure 7. *Month-long strain behaviour of individual inner and outer sensors (a-d), illustrating sensor-specific variations and differences between internal and external positions.*

A broader analysis was then performed for the month of June, covering a longer time span of three months-the first time such an extended dataset was available for processing (Figure 8). Over this three-month period, it is clearly shown that the sensor installed at position IN-2 experiences the highest overall strain. Furthermore, a gradual increase in strain levels is observed over time. This long-term trend indicates that continuous structural loading or environmental influences are affecting the monument progressively, reinforcing the value of long-duration monitoring.

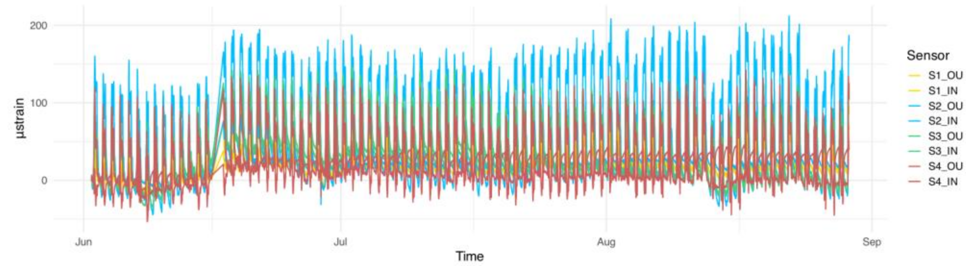

Figure 8. *Three-month strain evolution based on the June-August 2016 dataset.*

Finally, a comparison was conducted between the month of June in two consecutive years, June 2016 and June 2017, to assess the structure's behaviour over an annual cycle (Figure 9a - h). The results indicate that, although the initial and final deformation values differ only slightly, all sensors recorded marginally higher strain one year later, suggesting a small but measurable increase in structural loading at the perimeter wall. The same month was selected in both years to ensure comparable temperature conditions and visitor activity patterns, thereby allowing for a more reliable assessment of long-term strain behaviour.

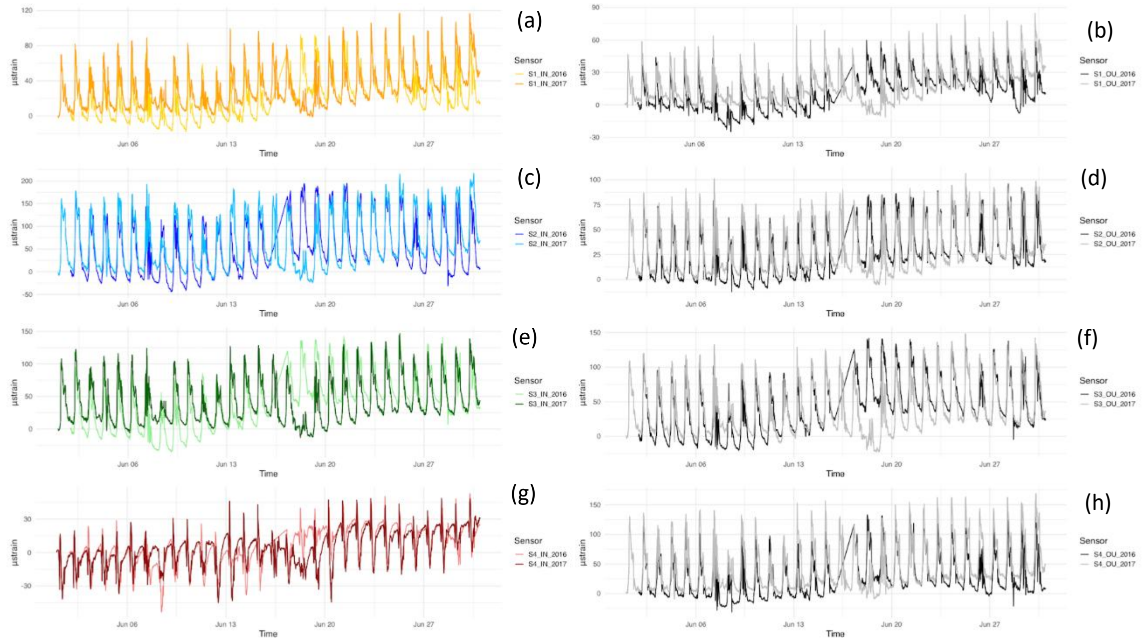

Figure 9. *Strain measurements for June 2016 and June 2017 (a-h) for all inner and outer sensors.*

CONCLUSIONS

The study has shown that the use of FBG sensors in a dense monitoring network enables the measurement of strain and temperature, providing detailed data on the structural response of the Acropolis Circuit Wall. To manage the very large dataset generated by these high-frequency measurements, a tailored data-processing workflow was developed. The raw time-series readings, captured every second by 10 sensors for almost two years, required specialised ingestion and visualisation tools, leading to the adoption of R for its statistical analysis strengths and efficient time-series data processing libraries. A custom pipeline parsed sensor output files, producing monthly data frames of about 2.3 million rows, from which temperature-corrected strain values were computed using vectorised operations. The data were then down-sampled through 20-minute moving-average windows and stored in compact binary format to support rapid re-analysis.

The results indicate that thermal effects significantly influence raw strain measurements, highlighting the necessity of thermal compensation. Inner and outer sensor positions capture different aspects of local structural behaviour, with certain sensors consistently exhibiting higher strain, reflecting the heterogeneous response of the wall to environmental and operational loads. The observed variation between the upper and lower sensors reflects a non-uniform deformation profile along the wall height, fully consistent with the static behaviour of the structural element. The structure consists of a retaining wall with buttresses which extends from position S3 downward. As a result, the upper part of the wall exhibits greater mobility than the lower part, an effect further amplified near the base where the S4 sensors are located close to a fixed support. Short-term analyses further show that sensor readings are affected by daily conditions, including visitor activity, while comparisons between “in” and “out” measurements reflect local bending behaviour combined with the influence of pre-existing cracks. In this context, the inner side captures transverse expansion of the structure, including joints and cracks, resulting in higher elongation values, while near-zero nighttime readings indicate that these strains are reversible as the wall is unloaded from daytime loads.

Overall, the study emphasises the importance of continuous high-resolution monitoring combined with systematic data management, particularly for large datasets. This approach provides a scalable and transferable methodology that can be applied to a wide range of historic monuments and complex structural systems. In this context, optical fibre sensor networks represent an effective solution for long-term structural health monitoring, supporting early damage detection and improving the understanding of structural behaviour in heritage masonry structures.

REFERENCES

Ambraseys, N. (2010). On the long-term seismicity of the city of Athens. *Proceedings of the Academy of Athens, Vol. A*, 81–136.

Bado, M. F., & Casas, J. R. (2021). A review of recent distributed optical fiber sensors applications for civil engineering structural health monitoring. *Sensors, 21*(5), 1818.

Henderson, T., & Fulcher, B. D. (2022). Feature-based time-series analysis in R using the theft package. *arXiv*.

Higgins, M., & Higgins, R. (1996). *A geological companion to Greece and the Aegean*. London: Gerald Duckworth & Co., 26–31.

Kalogeras, I., Stavrakakis, G., Melis, N., Loukatos, D., & Boukouras, K. (2010). The deployment of an accelerographic array on the Acropolis hill area: Implementation and future prospects. *Proceedings of a One-Day Conference, Modern Technologies in the Restoration of the Acropolis, Athens, Greece*, 39–42.

Kapogianni, E., & Sakellariou, M. G. (2025). Applications of optical fiber sensors in geotechnical engineering: Laboratory studies and field implementation at the Acropolis of Athens. *Sensors: Optical Fiber Sensors Used for Civil Engineering, 25*, 1450.

Kapogianni, E., Psarropoulos, P. N., Kokoris, D., Kalogeras, I., Michalopoulou, D., Eleftheriou, V., & Sakellariou, M. (2021). Impact of local site conditions on the seismic response of the Athenian Acropolis Hill. *Geotechnical and Geological Engineering, 39*(3), 1817–1830.

Kapogianni, E., Kalogeras, I., Psarropoulos, P., Eleftheriou, V., & Sakellariou, M. (2019). Suitability of optical fibre sensors and accelerographs for the multi-disciplinary monitoring of a historically complex site: The case of the Acropolis Circuit Wall and Hill. *Geotechnical and Geological Engineering, 37*(5), 4405–4419.

Kapogianni, E., Kalogeras, I., Psarropoulos, P. N., Giokaris, S., & Sakellariou, M. (2016). Structural health monitoring of the Athenian Acropolis’ walls via optical fibre sensors, accelerographs and numerical simulations. In K. Van Balen & E. Verstrynge (Eds.), *Structural analysis of historical constructions: Anamnesis, diagnosis, therapy, controls* (pp. 701–707). CRC Press, Taylor & Francis Group.

Koukis, G., Pyrgiotis, L., & Kouki, A. (2015). The Acropolis Hill of Athens: Engineering geological investigations and protective measures for the preservation of the site and the monuments. In *Engineering Geology for Society and Territory - Volume 8* (pp. 89–93).

Sakellariou, M., Kapogianni, E., Kalogeras, I., & Psarropoulos, P. (2016). Investigation of structural behaviour of the perimetric wall of the Athens Acropolis against seismic loads, via combined instrumented monitoring with optical fibre sensors and accelerographs. *Scientific Project Report, John Latsis Public Benefit Foundation*

Shumway, R. H., & Stoffer, D. S. (2017). *Time series analysis and its applications: With R examples* (4th ed.). Springer.

Soga, K., Kwan, V., Pelecanos, L., Rui, Y., Schwamb, T., Seo, H., & Wilcock, M. (2015). The role of distributed sensing in understanding the engineering performance of geotechnical structures. In *Geotechnical Engineering for Infrastructure and Development, XVI ECSMGE* (pp. 13–48). ICE Publishing.

Trikkalinos, I. K. (1977). Remarks on the published study on the geology of the Acropolis. *Proceedings of the Academy of Athens, 12–05*, 311–342.

Zambas, C., Ambraseys, N., Boletis, C., & Zamba, I. (2011). The two Choragic columns of the south slope of the Acropolis, as witnesses of the seismic history of the centre of Athens. *Scientific Project Report, John Latsis Public Benefit Foundation*.